Supporting Information

An Anion Metal-Organic Framework with Lewis Basic Sites-rich towards Charge-Exclusive Cationic Dyes Separation and Size-Selective Catalytic Reaction

Xu-Sheng Wang,[a,b] Jun Liang,[a] Lan Li,[a] Zu-Jin Lin,[a] Partha Pratim Bag,[a] Shui-Ying Gao,[a] Yuan-Biao Huang*[a] and Rong Cao*[a]

[a] State Key Laboratory of Structural Chemistry, Fujian Institute of Research on the Structure of Matter, Chinese Academy of Sciences, Fuzhou, Fujian, 350002, China. E-mail: ybhuang@fjirsm.ac.cn, rcao@fjirsm.ac.cn, Fax: (+86)-591-63173153, Tel: (+86)-591-63173153.

[b] University of the Chinese Academy of Sciences, Beijing, 100049, China.

Experimental section

1. Instrument for characterization

Elemental analyses (C, H, and N) were carried out on an Elementar Vario EL III analyzer. Powder X-ray diffraction (PXRD) data were collected on a Rigaku MiniFlex 600 diffractometer working with Cu Kα radiation, and the recording speed was 5° min^{-1} over the 2θ range of 5−50° at room temperature. Thermogravimetric analyses

(TGA) were recorded on a NETZSCH STA 449C unit at a heating rate of 10 ℃ min^{-1} under flowing nitrogen atmosphere. ^1H NMR spectra were recorded at ambient temperature on a BrukerAvance III spectrometer; the chemical shifts were referenced to TMS in the solvent signal in d_6-DMSO. The simulated powder patterns were calculated using Mercury 2.0. The purity and homogeneity of the bulk products were determined by comparison of the simulated and experimental X-ray powder diffraction patterns. UV-Vis absorption spectra were recorded on a quartz slide with a Lambda 35 spectrophotometer (Perkin Elmer, USA).

Crystallographic data of **FJI-C2** was collected on an Oxford diffractometer (Cu kα, λ = 1.54178 Å). The structures were solved by direct methods and refined by full-matrix least-squares calculations (F2) by using the SHELXTL-97 software. Because guest molecules $[(CH_3)_2NH_2]^+$ in the channels were highly disordered and could not be modeled properly, the SQUEEZE routine of PLATON was applied to remove their contributions to the scattering. The reported refinements are of the guest-free structures obtained by the SQUEEZE routine, and the results were attached to the CIF file. PLATON/SQUEEZE were employed to calculate their contributions to the distorted molecules and given a set of guest-free diffraction intensities. The structures were then refined again using the generated data. Crystallographic data of **FJI-C2** are summarized in Table S1. Selected bond distances (Å) and angles (°) for **FJI-C2** are summarized in Table S2.

The qualitative analysis of various substrates and products in Knoevenagel condensation reaction were carried out by a gas chromatograph (Angilent G7890A)

equipped with a FID detector. The compounds were separated by a HP-5 capillary column (30m×0.32mm ×0.25μm film thickness). The GC parameters were as follows: split ratio, 20:1; injector port temperature, 300°C; detector temperature, 300°C; injection volume, 1.0 μL. The oven temperature was initially set at 50 °C and held at this temperature for 5 min, then increased to 120°C at a ramp of 10°Cmin^{-1}, immediately increased to 300 °C at a ramp of 15°C min^{-1}. High purity nitrogen gas was used as a carrier gas at a flow rate of 20 mL min^{-1}. In this analysis, n-dodecane was used as an internal standard.

2. Coordination environment of FJI-C2

Interestingly, the independent Cd centers show different coordinate numbers. The Cd1 and Cd3 center exhibit similar 8-coordinated distorted tetrahedral geometry, (Cd1 binds with L1 via carboxylate O atoms and Cd3 binds with L1 and L2 in similar way). The Cd2 center exhibits a 7-coordinated distorted tetrahedral geometry, bind with L1 and L2. The Cd4 center exhibits a 6-coordinated distorted tetrahedral geometry, bind with L2 and two O-atoms from water. The L1 bridged to six Cd ions

(two Cd1, two Cd2 and two Cd3), thus acting as a 6-connected octahedral node. Two L2 are coordinated with two Cd4, which compose an 8-connected node (four Cd2 and four Cd3). Over all, the Cd1, Cd2, and Cd3 center that connected with four –COO- groups can be simplified into 4- connected nodes, separately, the two Cd4 together with two L2 can be served as an 8-connected node and the L1 which did not coordinated with Cd4 atoms can be seen as a 6-connected node.

3. Tables and Figures

Table S1 Crystal data and structure refinements for compound **FJI-C2**.

Compound	**FJI-C2**
Molecular formula [a]	$C_{108}\ H_{34}\ Cd_7\ N_{24}\ O_{52}$
Mr [a]	3286.39
crystal system	tetragonal
Space group	P -42_1c

a/Å	32.9676(3)
b/Å	32.9676(3)
c/Å	26.6956(4)
V, $Å^3$	29014.4(6)
Z	4
D, g/cm^3	0.755
GOF on F^2	0.955
R1 [$I>2\sigma(I)$]	0.0522
wR2 (all data)	0.1509
F(000)	6408
Flack	-0.041(6)
CCDC number	1430722

Distorted $[(CH_3)_2NH_2]^+$, DMF and crystaline H_2O were calculated by PLATON/SQUEEZE program, which is not shown in final formulae in CIF files.

Table S2 Selected bond distances (Å) and angles (°) for **FJI-C2**.

Cd(1)-O(4)#1	2.364(3)	Cd(3)-O(14)	2.291(3)
Cd(1)-O(4)	2.364(3)	Cd(3)-O(12)	2.343(4)
Cd(1)-O(1)	2.389(3)	Cd(3)-O(15)	2.363(5)
Cd(1)-O(1)#1	2.389(3)	Cd(3)-O(17)	2.398(6)
Cd(1)-O(2)#1	2.392(3)	Cd(3)-O(18)	2.421(5)
Cd(1)-O(2)	2.392(3)	Cd(3)-O(16)	2.419(6)

Cd(1)-O(3)#1	2.400(3)	Cd(3)-O(13)	2.482(4)
Cd(1)-O(3)	2.400(3)	Cd(3)-O(11)	2.483(4)
Cd(2)-O(19)	2.254(6)	Cd(4)-O(20)	2.250(9)
Cd(2)-O(8)	2.324(4)	Cd(4)-O(23)	2.301(7)
Cd(2)-O(9)	2.334(4)	Cd(4)-O(21)	2.357(8)
Cd(2)-O(6)	2.345(3)	Cd(4)-O(24)	2.372(8)
Cd(2)-O(10)	2.408(4)	Cd(4)-O(25)	2.380(13)
Cd(2)-O(7)	2.392(3)	Cd(4)-O(22)	2.512(15)
Cd(2)-O(5)	2.404(3)		

O(4)#1-Cd(1)-O(4)	88.87(17)	O(12)-Cd(3)-O(16)	85.29(17)
O(4)#1-Cd(1)-O(1)	121.41(13)	O(15)-Cd(3)-O(16)	54.03(16)
O(4)-Cd(1)-O(1)	121.94(13)	O(17)-Cd(3)-O(16)	152.88(17)
O(4)#1-Cd(1)-O(1)#1	121.94(13)	O(18)-Cd(3)-O(16)	98.26(18)
O(4)-Cd(1)-O(1)#1	121.41(13)	O(14)-Cd(3)-O(13)	54.00(12)
O(1)-Cd(1)-O(1)#1	85.31(16)	O(12)-Cd(3)-O(13)	134.99(12)
O(4)#1-Cd(1)-O(2)#1	85.16(14)	O(15)-Cd(3)-O(13)	81.29(17)
O(4)-Cd(1)-O(2)#1	84.58(14)	O(17)-Cd(3)-O(13)	80.42(16)
O(1)-Cd(1)-O(2)#1	139.85(11)	O(18)-Cd(3)-O(13)	121.40(18)
O(1)#1-Cd(1)-O(2)#1	54.54(11)	O(16)-Cd(3)-O(13)	121.71(16)
O(4)#1-Cd(1)-O(2)	84.58(14)	O(14)-Cd(3)-O(11)	134.10(13)
O(4)-Cd(1)-O(2)	85.16(14)	O(12)-Cd(3)-O(11)	54.84(12)
O(1)-Cd(1)-O(2)	54.54(11)	O(15)-Cd(3)-O(11)	82.41(16)
O(1)#1-Cd(1)-O(2)	139.85(11)	O(17)-Cd(3)-O(11)	74.39(18)

O(2)#1-Cd(1)-O(2)	165.61(16)	O(18)-Cd(3)-O(11)	115.22(17)
O(4)#1-Cd(1)-O(3)#1	54.35(12)	O(16)-Cd(3)-O(11)	121.63(15)
O(4)-Cd(1)-O(3)#1	143.21(12)	O(13)-Cd(3)-O(11)	80.20(11)
O(1)-Cd(1)-O(3)#1	83.81(13)	O(19)-Cd(2)-O(8)	84.7(2)
O(1)#1-Cd(1)-O(3)#1	83.30(13)	O(19)-Cd(2)-O(9)	154.0(3)
O(2)#1-Cd(1)-O(3)#1	90.66(14)	O(8)-Cd(2)-O(9)	94.81(17)
O(2)-Cd(1)-O(3)#1	91.53(15)	O(19)-Cd(2)-O(6)	106.0(3)
O(4)#1-Cd(1)-O(3)	143.21(12)	O(8)-Cd(2)-O(6)	140.42(13)
O(4)-Cd(1)-O(3)	54.35(12)	O(9)-Cd(2)-O(6)	90.90(14)
O(1)-Cd(1)-O(3)	83.30(13)	O(19)-Cd(2)-O(10)	99.0(4)
O(1)#1-Cd(1)-O(3)	83.81(13)	O(8)-Cd(2)-O(10)	84.81(15)
O(2)#1-Cd(1)-O(3)	91.53(15)	O(9)-Cd(2)-O(10)	55.18(15)
O(2)-Cd(1)-O(3)	90.66(14)	O(6)-Cd(2)-O(10)	128.90(14)
O(3)#1-Cd(1)-O(3)	162.44(18)	O(19)-Cd(2)-O(7)	112.4(3)
O(14)-Cd(3)-O(12)	171.00(13)	O(8)-Cd(2)-O(7)	55.03(13)
O(14)-Cd(3)-O(15)	92.42(17)	O(9)-Cd(2)-O(7)	87.91(15)
O(12)-Cd(3)-O(15)	90.04(18)	O(6)-Cd(2)-O(7)	86.19(12)
O(14)-Cd(3)-O(17)	93.25(19)	O(10)-Cd(2)-O(7)	123.94(17)
O(12)-Cd(3)-O(17)	88.54(19)	O(19)-Cd(2)-O(5)	85.1(2)
O(15)-Cd(3)-O(17)	152.50(17)	O(8)-Cd(2)-O(5)	163.64(14)
O(14)-Cd(3)-O(18)	89.69(17)	O(9)-Cd(2)-O(5)	88.75(17)
O(12)-Cd(3)-O(18)	84.12(17)	O(6)-Cd(2)-O(5)	55.23(12)
O(15)-Cd(3)-O(18)	152.14(18)	O(10)-Cd(2)-O(5)	84.15(16)
O(17)-Cd(3)-O(18)	54.79(18)	O(7)－Cd(2)-O(5)	141.21(12)

O(14)-Cd(3)-O(16)	89.14(17)	

Symmetry transformations used to generate equivalent atoms: #1 -x+1,-y+1,z； #2 -y+1,x,-z+1； #3 y,-x+1,-z+1； #4 x,y,z+1； #5 x,y,z-1； #6 -y+1/2,-x+1/2,z+1/2； #7 -y+1/2,-x+1/2,z-1/2； #8 y,-x+1,-z； #9 -y+1,x,-z； #10 x+1/2,-y+1/2,-z-1/2； #11 x-1/2,-y+1/2,-z-1/2；

Table S3 Maximum adsorption capacity of Methylene Blue (**MB^+**) on various adsorbents

Adsorbent	Maximum Adsorption Capacity	Reference

	(mg/g)	
Zn-MOF	0.75	Chem. Eur. J. 2013, 19, 3639.
Hierarchically mesostructured MIL-101	21	CrystEngComm, 2012, 14, 1613.
Superabsorbent hydrogel	48	J. Colloid Interf. Sci., 2006, 301, 55.
Tea waste	85	J. Hazard. Mater., 2009, 164, 53.
Zn-DDQ	135	Inorg. Chem., 2014, 53, 7692.
MOF@graphite oxide	183	J. Mater. Chem. A, 2013, 1, 10292.
MIL-101(Al)	195	J. Mater. Chem. A, 2014, 2, 193.
MOF-235	252	J. Hazard. Mater. 2011, 185, 507.
$PW_{11}V$@MIL-101	371	Chem. Eur. J., 2014, 20, 6927.
ErCu-POM (Er-3)	391	Chem. Commun., 2015,51, 3336.
Graphene oxide sponge	397	Carbon, 2013, 59, 372.
Activated carbon	400	J. Hazard. Mater. 2006,

		134, 237.
Caulerpalentillifera	417	Bioresour. Technol. 2007, 98, 1567.
Poly(vinylidenefluoride)-derived activated carbon fibers	486	Carbon. 2001, 39, 207.
Co/NPC derived from ZIF-67	503	Small, 2014, 10, 2096.
Activated carbon produced from New Zealand coal	588	Chem. Eng. J. 2008, 135, 174.
MIL-100(Cr)	645	J. Mater. Chem. A, 2013, 1, 8534.
Ni-MOF	708	Chem. Commun., 2014, 50, 14674.
Co-MOF	725	Chem. Commun., 2014, 50, 14674.
MIL-100(Fe)	736	J. Mater. Chem. A, 2013, 1,8534.
Amino-MIL-101-Al	762	J. Mater. Chem. A. 2014, 2, 193.
ZJU-24	902	Chem. Commun., 2014, 50, 14455.
FJI-C2 (Cd-MOF)	**1323**	**In this work**

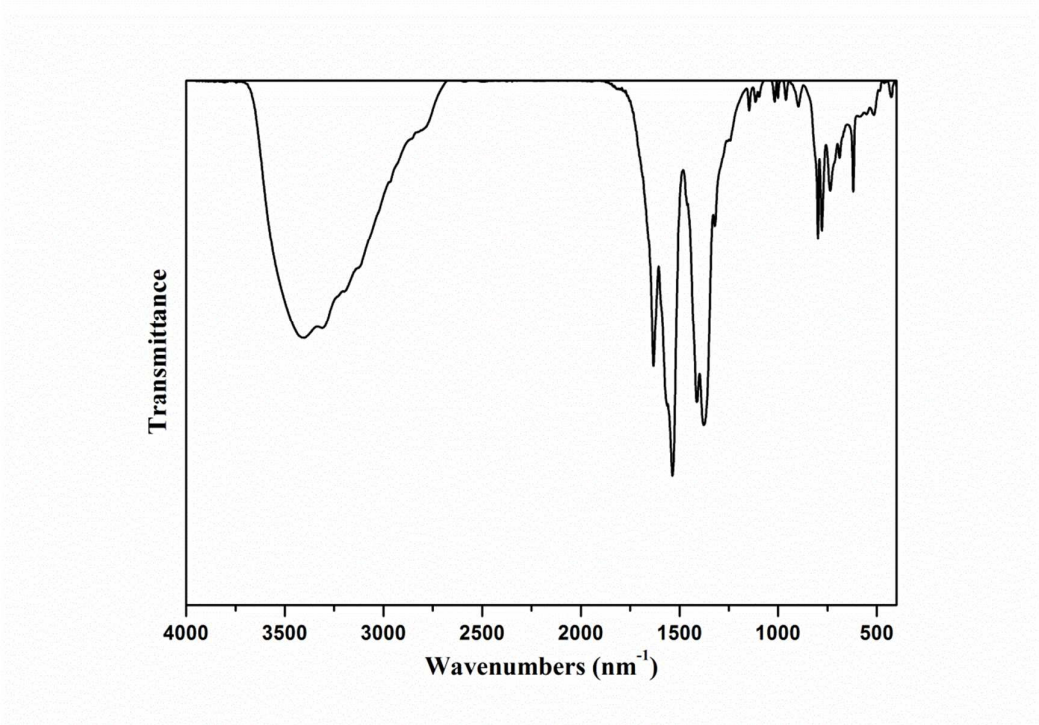

Figure S1. IR spectra of as-synthesized **FJI-C2**.

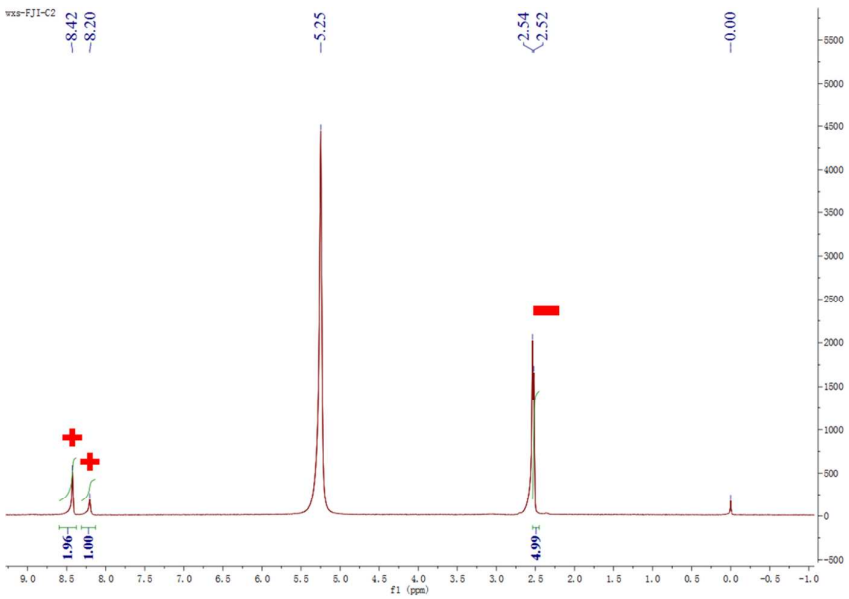

Figure S2 The ^{1}H-NMR spectrum of **FJI-C2** (washed with CH_2Cl_2 several times and dried under vacuum at room temperature) after digesting the as-prepared crystal with DMSO/DCl. Sign denoted with (✚) is assigned to H_6TDPAT, while the signs denoted with (▬) is assigned to $Me_2NH_2^+$ cations in the compound **FJI-C2**. According to the intensity integration, the ratio $Me_2NH_2^+$:H_6TDPAT is 2.5:1, which is consistent with the charge balance calculation.

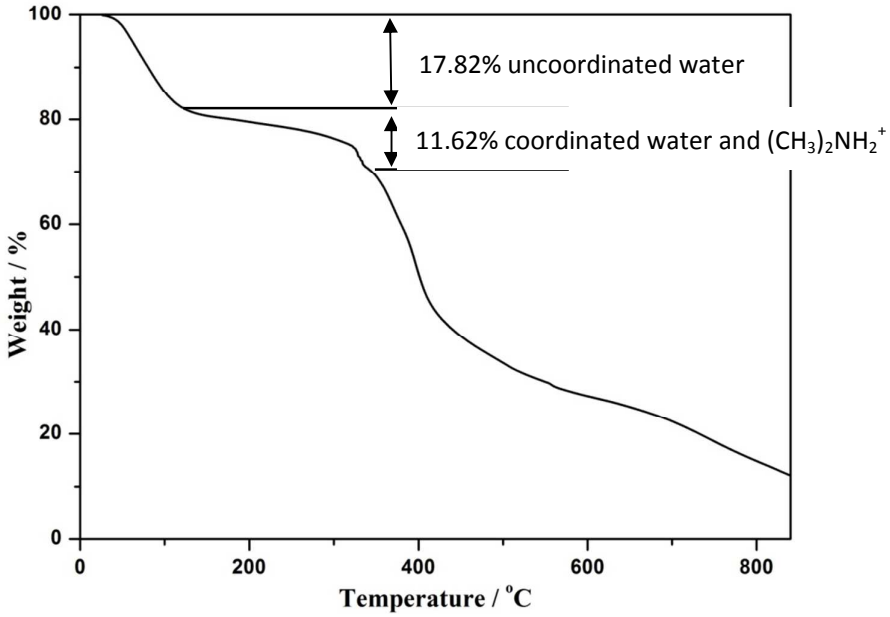

Figure S3. TG analysis of the as-synthesized **FJI-C2** measured under N_2 atmosphere from room temperature to 850 at the heating rate of 10 °C·min^{-1}.

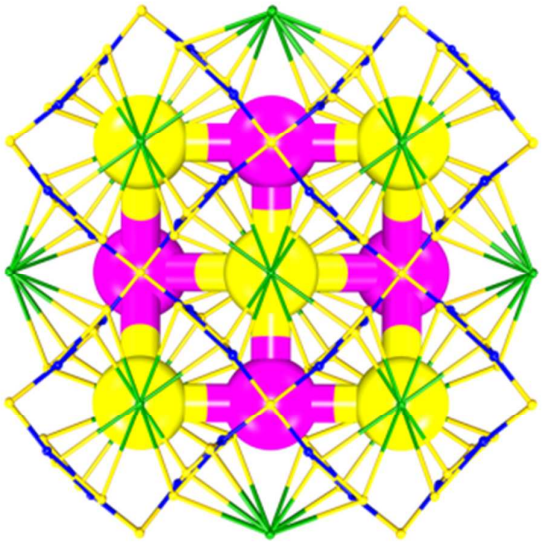

Figure S4 Topology analysis of **FJI-C2**. The colourful balls stand for the cages in **FJI-C2**.

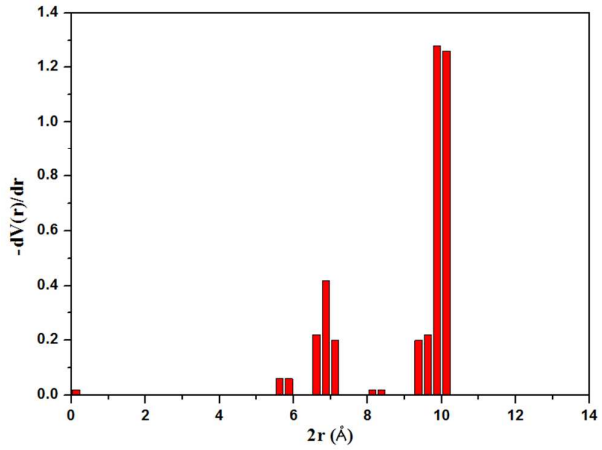

Figure S5 The size distribution of **FJI-C2** simulated by poreblazer _v3.0 software.

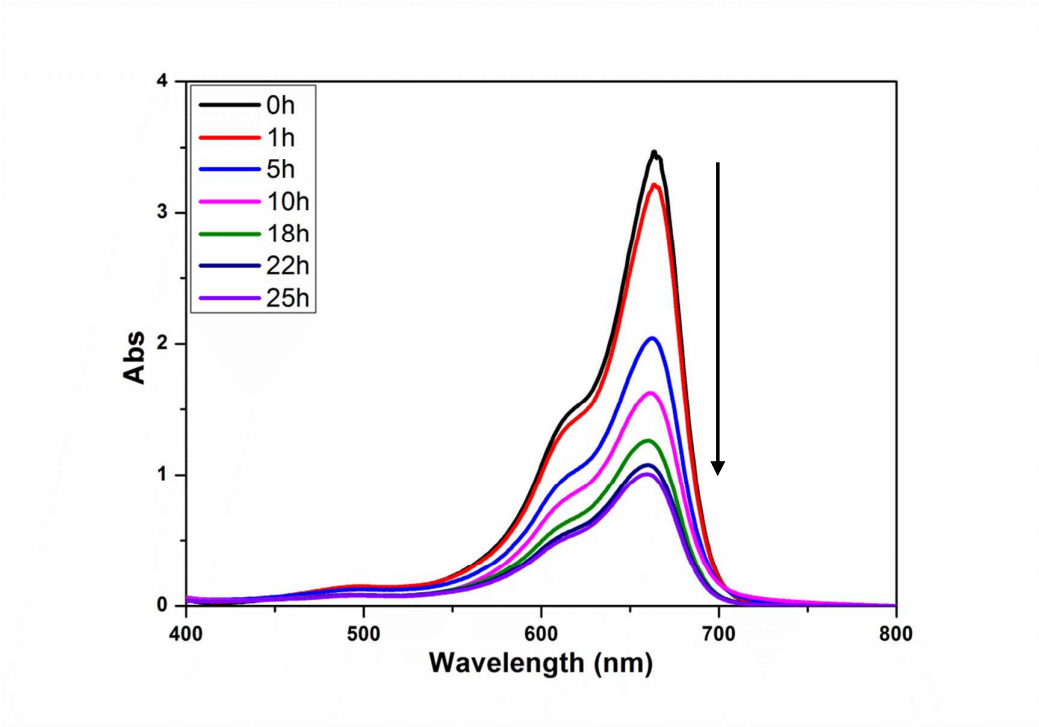

Figure S6 The UV absorption curve of $\mathbf{MB}^{+}$ by **FJI-C2** at a higher concentration of $\mathbf{MB}^{+}$.

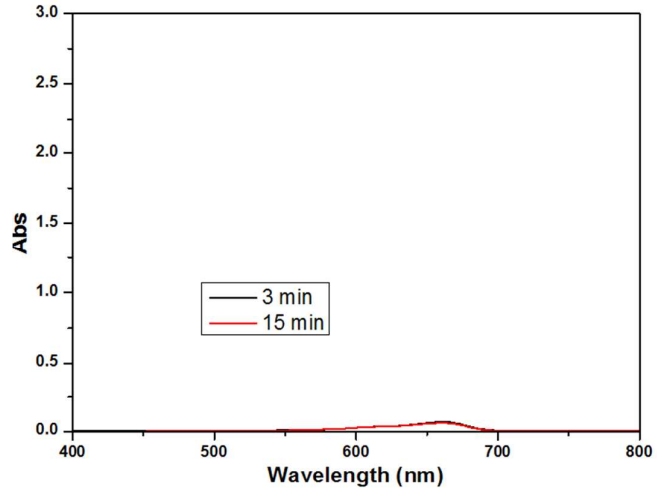

Figure S7 The UV-Vis absorption curve of MB^+ release from MB^+**@FJI-C2** in pure DMF solution.

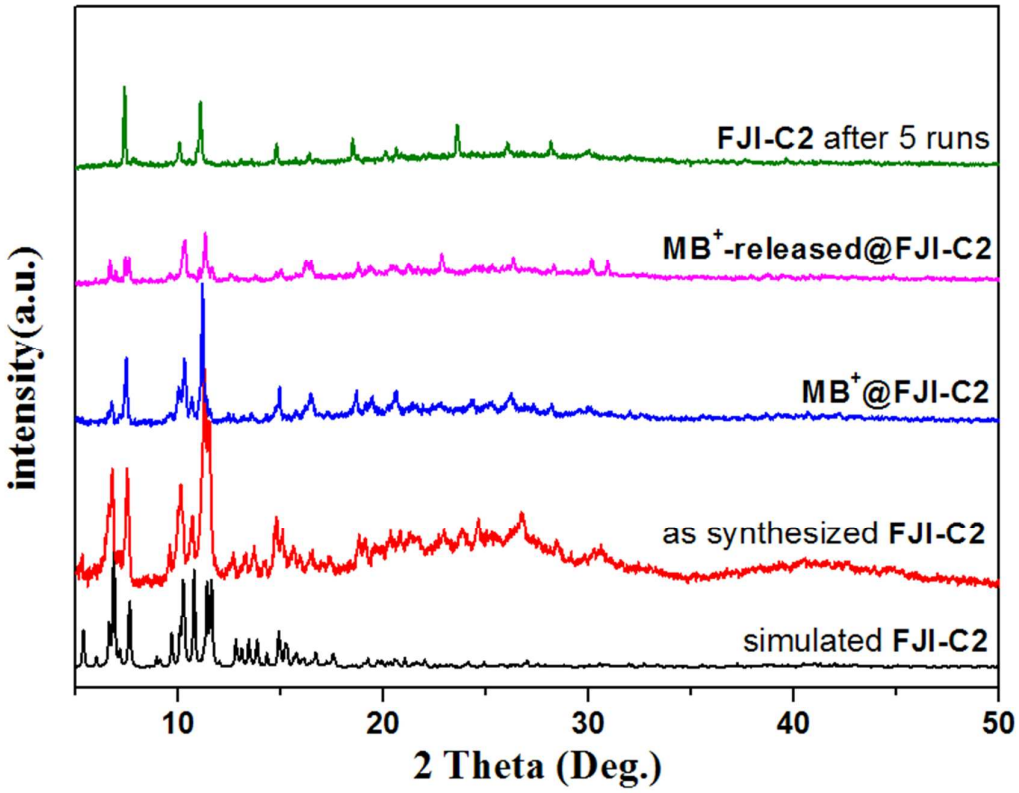

Figure S8 PXRD patterns for **FJI-C2**: simulated **FJI-C2**, as-synthesized **FJI-C2**, MB^+**@FJI-C2**, MB^+**-released@FJI-C2**, and **FJI-C2** after 5 runs.

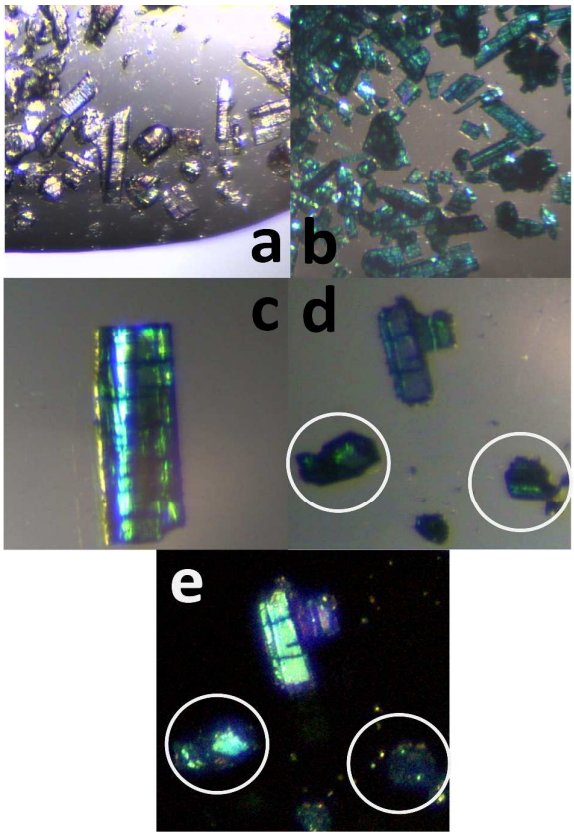

Figure S9 (a) **FJI-C2**, (b) **MB$^+$@FJI-C2**, (c) one rodlike **MB$^+$@FJI-C2**, (d) the cut **MB$^+$@FJI-C2**, and (e) the cut **MB$^+$@FJI-C2** under polarizedlight. The crystal in the white circle shows the cutting cross section of **MB$^+$@FJI-C2**.

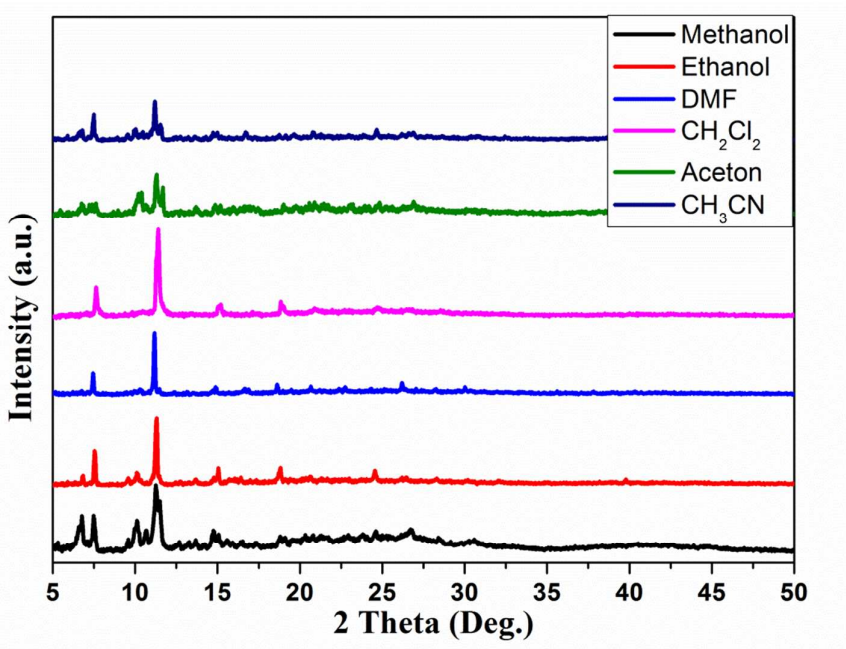

Figure S10 PXRD patterns for **FJI-C2** after immerged in different solvents for 24h.

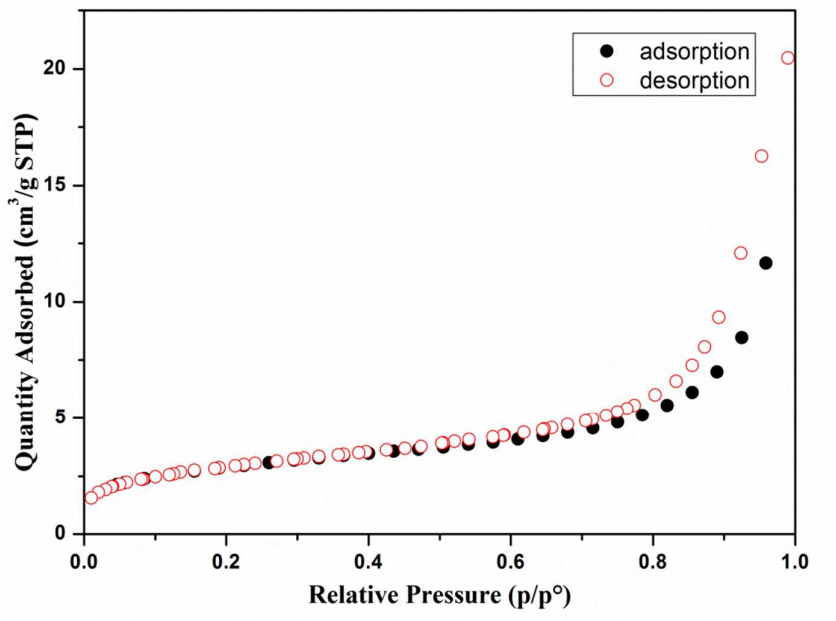

Figure S11 N_2 sorption isotherm of **FJI-C2**. The BET value is 10 m^2/g.